

Highlights

QBSD: Quartile-Based Seasonality Decomposition for Cost-Effective Time Series Forecasting

Ebenezer RHP Isaac, Bulbul Singh

- Live forecasting without the need for separate fit and predict.
- Computationally efficient compared to state-of-the-art methods.
- Simplified hyperparameter tuning with only two parameters.
- Evaluation with open and telecom datasets, comparing with the state of the art.
- Flexible time and day-dependent range estimation.

QBSD: Quartile-Based Seasonality Decomposition for Cost-Effective Time Series Forecasting

Ebenezer RHP Isaac^a, Bulbul Singh^a

^a*Global AI Accelerator (GAIA), Ericsson, Chennai, 600096, India*

Abstract

In the telecom domain, precise forecasting of time series patterns, such as cell key performance indicators (KPIs), plays a pivotal role in enhancing service quality and operational efficiency. State-of-the-art forecasting approaches prioritize forecasting accuracy at the expense of computational performance, rendering them less suitable for data-intensive applications encompassing systems with a multitude of time series variables. To address this issue, we introduce QBSD, a live forecasting approach tailored to optimize the trade-off between accuracy and computational complexity. We have evaluated the performance of QBSD against state-of-the-art forecasting approaches on publicly available datasets. We have also extended this investigation to our curated network KPI dataset, now publicly accessible, to showcase the effect of dynamic operating ranges that varies with time. The results demonstrate that the proposed method excels in runtime efficiency compared to the leading algorithms available while maintaining competitive forecast accuracy.

Keywords: Key Performance Indicator, forecasting, time series, machine learning, telecom AI

1. Introduction

Time series forecasting is of significant importance in research due to its wide range of applications not only within the field of telecommunications but across many different domains, such as forecasting sales data for seasonal items [1], in the energy industry to predict electricity demand as well as to forecast prices and market trends [2, 3], in finance, to predict stock prices, exchange rates, and other financial variables [4], in healthcare, to predict disease outbreaks, hospital admissions, and patient outcomes [5, 6] among many others.

Research suggests several approaches proposed as potential solutions for time series forecasting. Traditional methods such as ARIMA [7] and SARIMA [8] have been widely used for forecasting, but recent advancements in machine learning (ML) have led to the development of more powerful and flexible techniques such as deep learning (DL) [9] and ensemble methods [10]. DL algorithms have gained prominence in time series forecasting, especially for long-horizon forecasting. The landscape of DL-based forecasting

Email addresses: ebenezer.isaac@ericsson.com (Ebenezer RHP Isaac), bulbul17110@gmail.com (Bulbul Singh)

methods includes transformers [11], recurrent neural networks (RNNs) [12] and various combinations of MLP (multi-layer perception) and convolutional neural network (CNN) [13] structures. These models have shown significant improvements in forecasting accuracy over traditional statistical models by capturing complex temporal dependencies and nonlinear patterns in the data. Due to their prevalence in literature, the forecasting approaches that involve any form of neural network are categorized as “neural forecasting methods.”

Despite the existence of numerous forecasting methods, ensuring both accuracy and computational efficiency remains a formidable challenge, particularly when dealing with anomalies or irregularities in time series data. The field continues to grapple with several unresolved issues such as predicting long-term trends, handling large-scale time series data, addressing missing values, and minimizing space and time complexity. The latter is especially important given that many time series forecasting methods involve computationally intensive algorithms, which may hinder their practical application. Moreover, several forecasting methods necessitate complex hyperparameter tuning, with grid search often employed to identify optimal parameters, albeit at a substantial computational expense. For instance, even a slight deviation in any of the four parameters of SARIMA could lead to an increased forecasting error.

Though neural forecasting methods are considered superior in recent literature, they are impractical for scenarios involving a system consisting of a large number of time series variables with a need for frequent retraining. Such cases are common in RAN (radio access network) applications, e.g., PM KPI anomaly detection, sleeping cell detection, cell traffic forecasting and load balancing. A standard cell in RAN can generate over 300 network performance management (PM) KPIs every 15 minutes. A typical RAN topology is composed of several thousand such cells. Depending on the use case, the solution can be expected to forecast over 300,000 time series variables every 15 minutes. Furthermore, forecasting is only part of the solution for the aforementioned use cases; the system needs to apply additional computation on top of the forecasted outcomes. Due to the dynamic nature of these KPIs and the possibility of drifts, the solution would also require periodic retraining. From a business perspective, there would be no financial gain in employing hundreds of dedicated GPUs/CPU to work continuously for the use cases concerned, making the viability of neural forecasting solutions questionable for such applications. Therefore, there is a compelling need for a computationally efficient forecasting approach that has comparable forecasting accuracy to neural forecasting methods.

This paper proposes QBSD (Quartile-Based Seasonality Decomposition)¹ to address the need for a computationally efficient forecasting for telecom applications. QBSD is a time series forecasting method that achieves high forecast accuracy with reduced time and space complexity. It is designed for rolling forecasts on live data and does not require a separate fit and predict stage. Instead, this method uses a

¹QBSD has been filed as a patent by Ericsson [14]

moving window approach that continuously updates the model parameters as new data becomes available. A comparative study of the suggested technique with several state-of-the-art and popular forecasting methods reveals that the proposed method is superior in runtime efficiency compared to the best available algorithms while still being competitive in forecast accuracy as indicated by MAE, MSE, and RMSE error metrics, and the R^2 coefficient.

The following are the significant contributions of this article:

1. Implementation of a computationally efficient rolling forecasting algorithm with only two simple hyper-parameters that follows a statistical approach with a forecasting accuracy that rivals neural forecasting approaches.
2. The proposed method also estimates the bounds that depict the operating range that varies with time. These bounds are exposed for interpretability.
3. Evaluation of the proposed work with the state of the art on publicly available datasets comparing both forecasting accuracy and execution time.
4. Evaluation on a telecom KPI dataset to further emphasise the applicability of the proposed method for RAN KPI use cases, and enable further research progression by making the dataset publicly available.

2. Related work

The spectrum of time series forecasting literature can be broadly divided into statistical approaches, neural forecasting, hybrid models and other ML-based techniques. This section reviews the literature along with their relative strengths and limitations.

2.1. Statistical Approaches

Traditional statistical models such as Autoregressive Integrated Moving Average (ARIMA) [7] and Seasonal ARIMA (SARIMA) [15] has been used widely in various domains such as forecasting the demand in the food industry [16], and have demonstrated promising performance in capturing linear trends and seasonality patterns. One of the most successful statistical models is Facebook (FB) Prophet [17] with the ability to incorporate the effect of holidays in business-level forecasting applications. Nevertheless, statistical models often struggle with non-linear and complex patterns, limiting their effectiveness in specific scenarios such as long-horizon forecasting. However, due to their simplicity and computational efficiency, they are still preferred over deep learning methods today for big data applications [18].

2.2. Neural Forecasting

The DeepAR proposed by Salinas et al. [19] is based on an autoregressive RNN that can model the distribution of future values given past observations. NeuralProphet [20] uses a variant of RNN to capture

temporal dependencies in time series data and provides uncertainty estimates for the forecasts. The authors claim that NeuralProphet outperforms Prophet and is capable of handling large-scale datasets.

The transformer architecture has been adapted for time series forecasting to yield competitive results. Lim et al. [21] proposed a Temporal Fusion Transformer (TFT), an attention-based design that combines high-performance multi-horizon forecasting with comprehensible insights into temporal dynamics. The study in [22] proposes the utilization of CNN for local processing and a sparse attention mechanism to increase the size of the receptive field during forecasting. The Crossformer [23] is a recent transformer-based architecture that captures cross-dimension dependency using dimension-segment-wise embedding, a two-stage attention layer and a hierarchical encoder-decoder.

N-BEATS (Neural Basis Expansion Analysis for interpretable Time Series forecasting) [24] is a popular deep neural architecture based on backward and forward residual links with multiple stacks of MLP constructs (multi-layer FC) with ReLU nonlinearities. N-HiTS [25] is a recent improvement over N-BEATS through multi-rate sampling and multi-scale hierarchical interpolation but retaining the base stacked MLP structure.

Regardless of the type of neural approach adopted, DL models generally require extensive computational resources and longer training times limiting their practical applicability for large-scale production applications with resource constraints. Though successive models claim to be more computationally efficient than their predecessors, DL models cannot be as efficient as their statistical counterparts.

2.3. Hybrid Models

Hybrid models aim to combine the strengths of multiple forecasting techniques to improve overall performance. Serdar Arslan [26] proposed a hybrid LSTM and prophet model for forecasting energy consumption. The prophet model is applied to the original data to maintain seasonality, and bidirectional stacked LSTM is developed for decomposed time series data to lessen the impact of irregular patterns. Spranger et al. [27] proposed a bidirectional temporal convolutional network (BiTCN) that requires fewer parameters than the conventional Transformer-based approach. The study shows that BiTCN is more computationally efficient than the commonly used bidirectional LSTM. Abbasimehr et al. [28] combined LSTM, GRU and CNN with statistical methods for COVID-19 forecasting. Zheng et al. [29] compared the performance of recent hybrid models for traffic prediction. The study concluded that the parallelized architecture outperforms the stacked architecture, and models that can extract dynamic spatial features outperform models that focus solely on dynamic temporal feature analysis.

The drawback of hybrid models is the increased complexity in model design and parameter tuning. Integrating multiple models requires careful selection and optimization of individual model components, alongside determining the optimal weighting scheme for combining their predictions. Additionally, hybrid models may introduce additional computational overhead as combining different algorithms requires more

computational resources than single-model approaches. While there are approaches like BiTCN that consider reducing the computational overhead, studies like [30] forego the consideration of computational complexity altogether by building a framework to learn a weighted combination of multiple statistical, ML-based and neural forecasters.

2.4. Other ML Techniques

Berry et al. [31] proposed a Bayesian approach to estimate consumer sales. The study arose from the realization that the variability observed in high-frequency sales is due to the compounding impact of variability in the number of transactions and sales-per-transaction. BayesMAR is a simple strategy of extending the traditional AR model to a median AR model (MAR) for time series forecasting is proposed in [32].

In [33] Januschowski et al. described why tree-based methods were so popular in the M5 competition. The paper discussed software packages that employ gradient boosting models, including LightGBM [34] and XGBoost [35], which have demonstrated robustness and high performance. Tree-based models can be preferred over DL models for data-intensive applications since they are far superior in computational efficiency. However, tree-based models require careful tuning of hyperparameters as they may be prone to overfitting, especially when dealing with noisy or sparse data.

In summary, several strategies, ranging from conventional statistical models to more modern ML-based techniques, have been presented for time series forecasting. While existing forecasting methods have progressed in tackling various challenges, some issues remain unresolved. These issues include the requirement for complicated hyperparameter tuning and separate fit and prediction stages in existing methods which result in high computational costs. Existing literature has yet to cover the aspect of the operating range of values that varies with time. This phenomenon is mostly seen in telecom data wherein the standard deviation of the data is higher during the day and lower close to midnight.

3. Method

The target architecture of the proposed method was designed based on the following criteria

1. Rolling forecast model. The target use cases concern time series data that are highly dynamic and require an updated context for each prediction. A rolling forecast that does not require a separate fit and predict step is ideal for this setting.
2. Minimal parameters for functioning. Fewer parameters will allow for a simpler design, reduce overfitting, faster training and inference, and generalize with minimal training data.
3. Minimal hyperparameters to tune without the need for complicated optimization mechanisms. Fewer hyperparameters also allow for better model consistency.

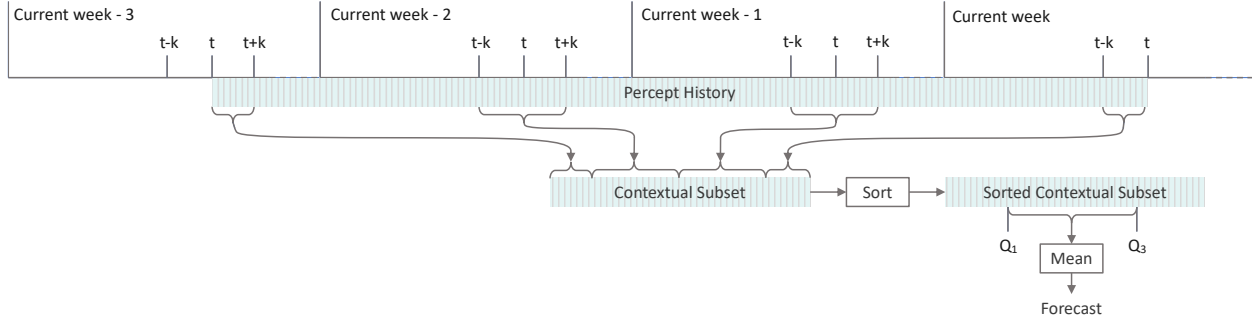


Figure 1: Schematic architecture of QBSD forecast computation, where t is the current timestamp and k is the context period.

4. Ability to estimate operating range that varies with time. E.g., value ranges observed closer to midday are much greater than midnight. Having this information available can enable the user to make better-informed decisions.
5. Prioritize computational efficiency and interpretability while retaining a forecasting accuracy that can compete against neural forecasting approaches

3.1. QBSD Algorithm

The basic version of QBSD addresses daily and weekly seasonality by assessing the historical patterns of the past month. It is designed for rolling forecasts on live data while holding a context window of 4 weeks. In other words, the system maintains a first-in, first-out (FIFO) buffer containing a rolling 28-day window of time series data, updated with each data point captured in the stream. Only a subset of context window holds the most relevant information to forecast the value for the next timestamp. This subset is called the *contextual subset*. The contextual subset is built based on the following assumptions.

1. At any given time of the day, the values corresponding to timestamps closest to the timestamp to be forecasted provide a better contribution to estimating the forecast value than the other timestamps.
2. The data distribution on a given day of the week is similar to the same day of the week for the most recent weeks.

The contextual subset compilation and forecasting operation is clearly illustrated in Fig. 1. Let

t denote the timestamp for which the forecasted value is to be determined,

k represent the *context period*, indicating the number of timestamps closest to t that are to be taken into consideration,

$day(t)$ be the day of week corresponding to t ,

$week(t)$ be the week of the year corresponding to t ,

$M(t)$ symbolize the value of series M at t , and

S denote the contextual subset.

Algorithm 1 succinctly explains the QBSD forecasting technique. Considering t to be the ‘current’ timestamp, S is compiled as follows: take the values $M(t - k)$ through $M(t - 1)$ for the current day, i.e., $day(t)$ in $week(t)$. Then take values from $M(t - k)$ through $M(t + k)$ of the same day for the past two weeks, $day(t)$ of $week(t) - 1$ and $week(t) - 2$. Finally, take $M(t)$ through $M(t + k)$ for $day(t)$ of $week(t) - 3$. The quartiles, Q_1 and Q_3 , are computed from S . The mean of the values that lie between these quartiles within S is the forecast for timestamp, t . The interquartile range, $IQR = Q_3 - Q_1$, becomes the expected deviation for timestamp, t

Algorithm 1 Quartile-Based Seasonality Decomposition

Require: Timestamp t , 1 month history of series M , context period size k

Compile contextual subset S from history (total of $6k + 3$ samples)

$M(t - k)$ through $M(t - 1)$ for $day(t)$ of $week(t)$

$M(t - k)$ through $M(t + k)$ for $day(t)$ of $week(t) - 1$ and $week(t) - 2$

$M(t)$ through $M(t + k)$ for $day(t)$ of $week(t) - 3$

Calculate quartiles Q_1 and Q_3 of S

$IQR = Q_3 - Q_1$

$forecast(t) = \text{mean}(x \mid x \in S \text{ and } Q_1 < x < Q_3)$

$difference_residual(M, t) = M(t) - forecast(t)$

$normalized_residual(M, t) = (M(t) - forecast(t)) / \max(IQR(t), c)$

return $Q_1, Q_3, IQR, forecast, residuals$

It is important to note that the value of the quartiles (and hence the resulting IQR) are different for each timestamp, hence deriving the expected operating range for each timestamp at any given time of the day; Q_1 depict the expected lower range whereas Q_3 depict the expected upper range. While the algorithm samples all values from time $t - k$ up to $t + k$ for the past two weeks, it only considers t to $t + k$ for the third week. This is because, in the current week, it is only possible to take values from time $t - k$ up to $t - 1$. The sampling is done so that no period would have an additional overlap bias while calculating the quartiles.

Two residuals can be calculated through the algorithm, namely, difference residual and normalized residual. The difference residual is obtained by computing the difference between the forecasted and predicted value for the corresponding timestamp. The normalized residual is the difference residual divided by the $\max(IQR, c)$ for the corresponding timestamp where c is the *contingency constant*. Either of them can be used based on the requirements of the use case. The dynamic operating range information is captured by

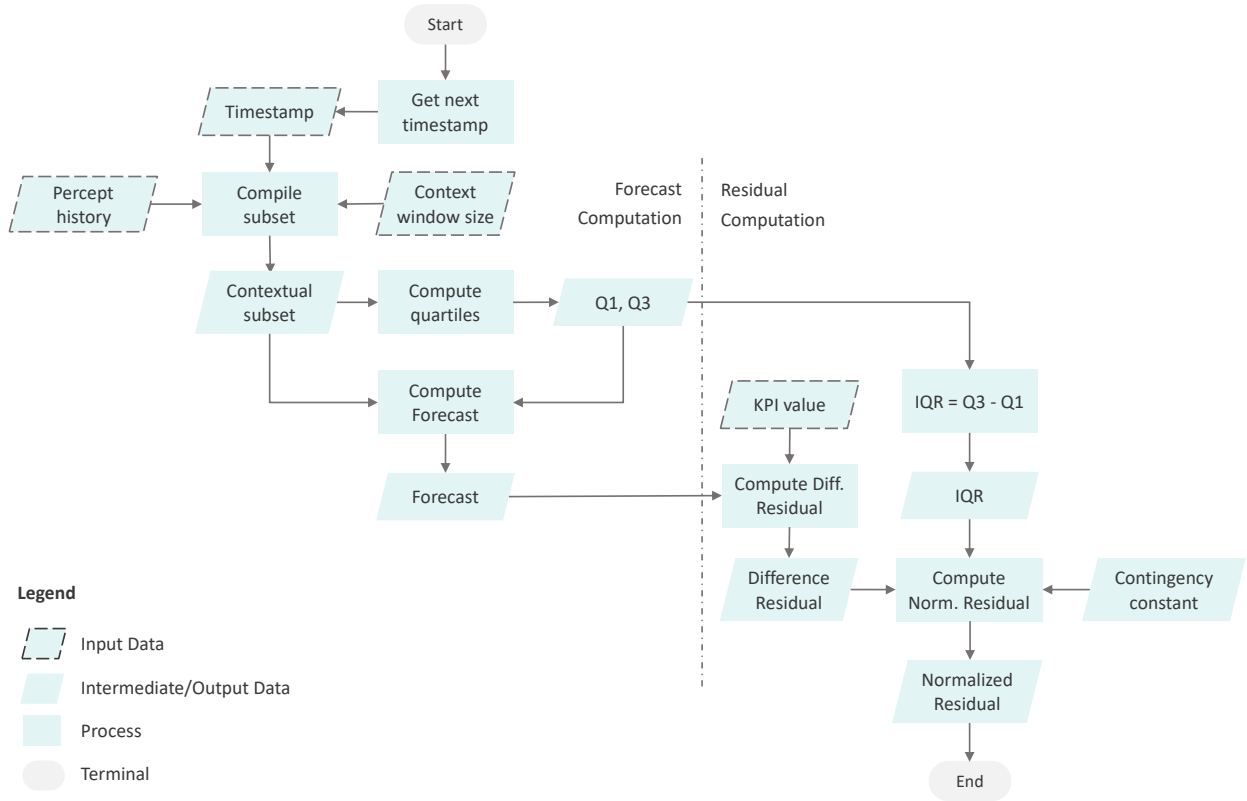


Figure 2: Flowchart illustrating QBSD. The flow begins with the input timestamp for which the forecast should be generated. This forecast along with the observed KPI value of the given timestamp is used for residual computation.

the normalized residual.

The flowchart for the QBSD method is depicted in Fig. 2. This chart includes the steps involved to generate the expected bounds (quartiles), forecast and residuals for a single timestamp. This process is repeated for every incoming timestamp in production.

Considering the mean of the elements between Q_1 and Q_3 as the forecast eliminates the possible outliers in the contextual subset. The normalized residual in this context normalizes the obtained residual with respect to the expected range at a given point in time. The contingency constant not only eliminates the possibility of a divide-by-zero error when $IQR = 0$, but also prevents the residual to be hypersensitive to lower ranges. For example, typical values of Active Uplink Users KPI usually range in the order of thousands for a densely-populated urban cell; during midnight, it is almost always 0. Hence, even a minor peak, such as 5, is considered a significant outlier in a statistical sense. However, when the operating range is so high, such a minor magnitude should not be considered an anomaly in a practical scenario. So, in this example, the value of c can be between 10 to 100 to avoid unnatural spikes in the normalized residual arising from nominal fluctuations in the time series data at lower expected ranges.

If the minor statistical deviation of values is important for the application concerned, then a nominal value could be $c = 1$ assuming the data domain consists of non-negative integers. In the general case, where such deviations are not important for the use case at hand, a better selection can be $c = |P_1(X)|$, that is, c can take an arbitrarily small value from the subset, such as 1-percentile of the entire range of values that X can exhibit. Hence, in practical usage, the value of c can be determined by computing $P_1(X)$ where P_1 computes 1-percentile of the training dataset denoted by X .

The proposed method implicitly handles seasonal variations, long-term secular trends and cyclic fluctuations to obtain irregular variations, but it does not consider short-term trends. This algorithm is specially designed for time series data which assumes a constant secular trend over the short term and that a sudden change in trend could be potentially anomalous. For example, network cells are limited in resources, and the solution must capture (not decompose) changes in trend when it comes to RAN KPIs to make appropriate business decisions.

While the basic version of QBSD as described accounts for daily and weekly seasonality, depending on the granularity of the data, the algorithm can be altered to capture monthly and yearly seasonality as well depending on the granularity of the data and the context window size. If the interval between each successive data point of the given dataset is one day, then the context period will be in the order of days and the context subset can be compiled by spanning between months or years depending on the requirement of the use case.

Since both the quartile series can be used as a visual aid for the operator to make informed decisions, these series can be smoothed before being plotted. The smoothing method that can be employed is a solution design choice. For example, it can be a Savitzky-Golay filter [36] or even a simple moving average.

3.2. Example

This section illustrates a short example of the QBSD application to a simple anomaly detection use case. Fig. 3 includes a snapshot of Active Uplink Users KPI over two months; only four weeks are shown here for

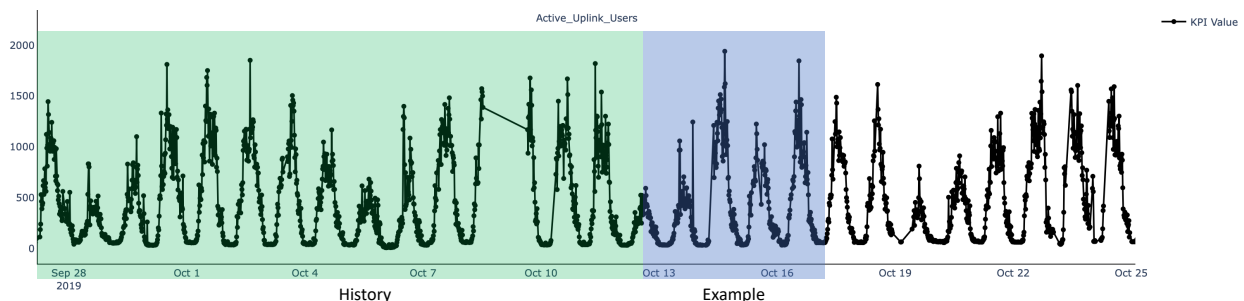


Figure 3: Sample input data. Percept history is highlighted in green while QBSD is performed on the example sequence highlighted in blue. Note that there can be missing data in history.

clarity. Note how the data follows both daily and weekly seasonal patterns. The cyclic pattern that occurs every day depicts daily seasonality. The periodic pattern of five consecutive daily peaks (corresponding to weekdays) followed by two smaller peaks (corresponding to weekends) depict weekly seasonality. Also note that this dataset contains missing data, e.g., between Oct 8, 12:30 and Oct 9, 15:45. Nevertheless, there were enough samples for the previous weeks for the same period to accurately estimate the forecast and range for that period. This data was passed through the QBSD algorithm to illustrate the seasonality decomposition. For this example, the context period was $k = 2.5$ hours and the contingency constant was $c = 1$.

Figure 4 shows the sample output of the algorithm. The output compares the QBSD forecast with the observed KPI data along with the generated normalized residual. The sample output shows that the proposed method has captured the lower and upper bound effectively. The variation between the expected lower and upper limits differed throughout the day. The range appeared narrower around midnight and broader during the day. The forecast also adequately approximated the expected value of the KPI. The general notion is that any value that deviates significantly beyond these bounds is probably an anomaly. In this case, the first two spikes and one dip qualified as anomalies. Not all KPI values that exceed the expected bounds can be considered anomalous. For instance, consider the third spike in this example: it was just above the expected range, but the normalized residual shows that the peak was not significantly greater than the others calculated in recent history. Hence, statistically, the third spike is not an anomaly, but this definition could differ from one use case to another based on the business requirements.

The severity of an anomaly in this example is inversely proportional to the expected range at the time of deviation. E.g., a moderate deviation at midnight can be considered anomalous while during the day, the deviation ought to be significantly large for it to be alerted as an anomaly.

3.3. Computational Complexity

The computational complexity of QBSD per forecast is derived by considering the number of elements in the input data used to compute the forecast. Let n be the number of elements in history fed to the algorithm. Only a subset consisting of m elements from the set of n elements is considered for computation (contextual subset), and the size of that subset is far lesser than n ($m \ll n/2$). Hence, $O(\log n)$ can represent the subset of elements that proceed to the next step. The quartile computation involves sorting by Quicksort, followed by subsetting and mean calculation for the forecast resulting in $O(m)$ time. Because $O(m)$ equates to $O(\log n)$, one can regard the resulting time complexity of QBSD as $O(\log n)$.

4. Experimental setup

4.1. Datasets

The evaluation included six open datasets to compare the performance of the proposed method with the state of the art. The following is a description of each dataset with the respective training and testing

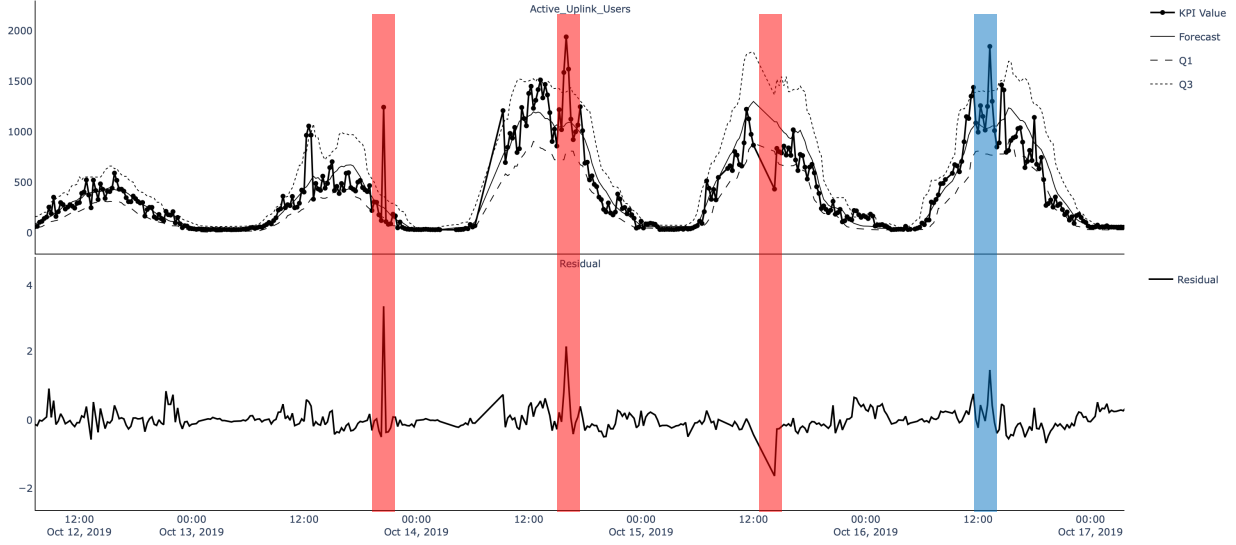


Figure 4: Illustration of QBSD applied on the example highlighted in Fig. 3 along with normalized residuals. Red bars indicate definitive anomalies wherein the blue bar indicates a peak that is not statistically an anomaly.

ranges. Table 1 summarises the statistics of each of these datasets.

Births2015 [37] comprises daily records documenting the birth rate observed in the year 2015. A moving training window of one month is employed to predict the next month of data (from 01-02-2015 to 28-02-2015).

Electricity Demand [38], also known as Daily Electricity Price and Demand Data, contains the electricity demand, price, and weather data in Victoria, Australia, over 2016 days from 01-01-2015 to 06-10-2020. A moving training window of one year is employed to predict one month of data (from 01-01-2016 to 31-01-2016).

Bitcoin Transactional Data [39] contains daily records on the number of Bitcoin transactions from July 2010 to July 2022. A moving training window of one month was employed to predict one year of data (from 01-01-2016 to 31-12-2016).

Electricity [40], also known as the Electricity Load Diagrams dataset from the UCI Machine Learning Repository, contains the electricity load consumption of 321 clients over three years. A moving training

Table 1: Dataset statistics and QBSD parameters

Dataset	No. of records	Frequency	Training window	Target	k
Births2015 [37]	365	daily	1 month	births	1 day
Electricity Demand [38]	2106	daily	1 year	demand	2 days
Bitcoin Transactional [39]	4389	daily	1 month	transactions	2 days
Electricity [40]	17520	hourly	1 year	MT_320	2 hours
Weather [41]	35064	hourly	1 year	WetBulbFahrenheit	2 hours
EON1-Cell-F [42]	8544	quarter-hourly	1 month	KPIs A to F	1 hour

Table 2: Methods included in the evaluation

Method	Reference	Approach	Year
SARIMA	Guin [8]	Statistical	2006
XGBoost	Chen and Guestrin [35]	Tree-based	2016
LightGBM	Guolin Ke et al. [34]	Tree-based	2017
Prophet	Taylor and Letham [17]	Statistical	2018
N-BEATS	Oreshkin et al. [24]	Neural	2019
N-HiTS	Challu et al. [25]	Neural	2022
QBSD	Proposed	Statistical	-

window of one year is employed to predict one month of data (from 01-01-2013 00:00:00 to 31-01-2013 23:00:00).

Weather [41] provides local climatological data for 1600 U.S. locations over four years from 2010 to 2013 at an hourly interval. A moving training window of one year is employed to predict one week of data (from 01-03-2011 00:00:00 to 07-03-2011 23:00:00).

EON1-Cell-F [42] is a synthetic dataset for univariate time series forecasting from the Ericsson Outlier Nexus (EON) compiled to represent the characteristics of Performance Management (PM) cell KPIs. This dataset is made publicly available by GAIA through Ericsson Research. It contains the data of 6 KPIs from February 2023 to April 2023 with a 15-minute interval between data points. The interval is considered the ROP (Result Output Period). Thus, there are 96 ROPs in a day. A moving training window of one month is employed to predict one month of data (from 01-04-2023 00:00:00 to 30-04-2023 23:45:00).

4.2. Baseline methods for comparison

The performance of QBSD is compared with the following state-of-the-art and popular forecasting methods. The summary of the methods is shown in Table 2.

4.2.1. Statistical models

SARIMA [15] is an extension of the ARIMA model to capture seasonal patterns in the data. Prophet [17] is a model developed by Facebook’s Core Data Science team that utilizes a decomposable time series model with three main components: growth, seasonality, and holidays. While these methodologies do not pertain to recent innovations, their enduring relevance persists in addressing contemporary business complexities and scholarly advancements. Furthermore, given that QBSD is also a statistical forecasting model, these methods inherently engage in direct juxtaposition with QBSD.

4.2.2. Tree-based models

XGBoost [35] is a gradient-boosting algorithm that combines multiple decision trees to generate forecasts. XGBoost uses a range of optimization techniques to minimize the loss function, including regularization

to prevent overfitting and early stopping to avoid unnecessary computation. LightGBM (Light Gradient Boosting Machine) [34] is designed to be faster and more memory efficient than XGBoost. It employs histogram-based gradient boosting in which data is bucketed into bins using a histogram of the distribution. The bins are used to iterate, calculate the gain, and split the data. It has also gained popularity in the M5 competition.

4.2.3. Neural forecasting models

N-BEATS [24] is based on a stack of fully connected layers that learn to decompose a time series into a set of basic functions, which are then used to generate forecasts. N-BEATS has achieved state-of-the-art results in several time series forecasting benchmarks, including the M4 competition. N-HiTS [25] is an improvement over the N-BEATS architecture through multi-rate sampling and multi-scale hierarchical interpolation.

4.3. Training procedure

The experiments are conducted on the datasets separately using the aforementioned methods and QBSD. To predict individual data points within the test set, each algorithm in this study utilized a moving training window, akin to the technique employed in QBSD. To facilitate this process, a multiprocessing pool was employed, with each selected method operating in parallel. N-BEATS and N-HiTS did not require the implementation of a moving train window since they were already designed for rolling forecasts.

Prophet was utilized with its default hyperparameters. For SARIMA, the optimal values for p , q , and seasonal components P , Q , and m were determined using the auto ARIMA function [43]. N-BEATS and N-HiTS were implemented using the darts package [44], the generic architecture of N-BEATS was utilized for the `Births2015` dataset and interpretable architecture for all the other datasets with varying input and output chunk lengths for each dataset. Both N-BEATS and N-HiTS were executed for 100 epochs for `Births2015`, `Electricity Demand`, and `Bitcoin Transactional` datasets, and 50 epochs for `EON1-Cell-F`, `Electricity` and `Weather` datasets. The learning rate, n estimators, and max depth for XGBoost and LightGBM were set to 0.01, 1000, and 3, respectively, for all datasets, along with early stopping rounds at 50.

For QBSD, the context period was set to $k = 1$ hour to compile the contextual subset using values from the current and the previous 3 weeks for `EON1-Cell-F`. A similar configuration was set for the `Bitcoin Transactional data` but with $k = 2$ days. To determine the most accurate forecast, the size of the context period was manually adjusted for each dataset, and the forecast is observed. For the `Births2015` dataset, $k = 1$ day with the contextual subset spanning the previous 5 weeks. `Electricity demand` data revealed both weekly and annual seasonality. In this case, $k = 2$ days with the contextual subset obtained from the previous two weeks of data for the given timestamp and the past year for the same timestamp. A similar

Table 3: MAPE comparison of forecasting approaches

Method	Datasets											Mean	p-value
	Births2015	Electr. Demand	Bitcoin Transact.	Electricity	Weather	EONI-Cell-F A	EONI-Cell-F B	EONI-Cell-F C	EONI-Cell-F D	EONI-Cell-F E	EONI-Cell-F F		
SARIMA	2.85	9.33	7.06	3.75	4.61	19.41	19.91	21.91	39.82	6.88	83.60	19.92	0.3188
XGBoost	1.11	3.48	2.96	1.02	5.38	5.46	6.60	5.48	7.16	2.14	13.07	4.90	1.0000
LightGBM	18.29	7.71	9.71	4.17	11.01	14.92	12.01	13.69	38.60	4.79	59.80	17.70	0.9584
Prophet	2.16	8.50	6.58	6.49	29.75	39.84	19.32	35.41	75.77	26.01	116.84	33.33	0.0122
N-BEATS	1.38	0.99	5.14	7.23	21.35	15.41	18.38	18.14	39.90	5.74	75.42	19.01	0.8398
N-HiTS	3.16	11.35	11.04	5.64	21.18	20.57	21.87	31.54	52.00	7.84	108.34	26.77	0.0004
QBSD	1.83	10.19	7.42	5.29	15.62	15.70	18.89	17.78	42.08	5.14	81.88	20.17	-

The p-values were obtained through a Wilcoxon signed-rank test comparing the particular method with the QBSD results. The alternative hypothesis posits that QBSD results have a lower MAPE than the corresponding method being tested.

configuration was also utilized for **Electricity** and **Weather** datasets as they both also demonstrated yearly seasonality with $k = 2$ days.

4.4. Metrics

The following metrics were used to evaluate the performance of each forecasting method: mean absolute error (MAE), mean squared error (MSE), root mean squared error (RMSE), mean absolute percentage error (MAPE), and R^2 statistics.

$$\begin{aligned}
 \text{MAE} &= \frac{1}{N} \sum_{i=1}^N |y_i - \hat{y}_i|, & \text{MSE} &= \frac{1}{N} \sum_{i=1}^N (y_i - \hat{y}_i)^2, \\
 \text{RMSE} &= \sqrt{\frac{1}{N} \sum_{i=1}^N (y_i - \hat{y}_i)^2}, & \text{MAPE} &= \frac{1}{N} \sum_{i=1}^N \frac{(y_i - \hat{y}_i)}{y_i} \times 100, \\
 R^2 &= 1 - \frac{\sum_{i=1}^N (y_i - \hat{y}_i)^2}{\sum_{i=1}^N (y_i - \bar{y})^2}.
 \end{aligned}$$

Here, N denotes the number of test instances, y_i and \hat{y}_i correspond to actual and forecast values for the instance i , respectively, and \bar{y} denotes the mean of the actual values.

5. Results and Discussion

This section provides an account of the experiment outcomes undertaken to compare the performance of QBSD with existing approaches. For brevity, Table 3 presents the MAPE results of these experiments, accompanied by corresponding p-values for statistical validation. Interested readers seeking a comprehensive

Table 4: Execution time* of each algorithm for training and single prediction

Method	Datasets						p-value
	Births2015	Electr. Demand	Bitcoin Transact.	Electricity	Weather	EON1-Cell-F	
SARIMA	1.03 s	8.71 s	278 ms	5.88 s	5.91 s	2.17 s	0.016
XGBoost	283 ms	376 ms	246 ms	316 ms	93.9 ms	246 ms	0.016
LightGBM	11.1 ms	17.3 ms	15 ms	88.8 ms	208 ms	120 ms	0.047
Prophet	891 ms	742 ms	1.08 s	4.47 s	6.81 s	4.63 s	0.016
N-BEATS	14 s	4.86 s	17.7 s	2 hr 2 s	13 min 20 s	3 min 17 s	0.016
N-HiTS	3.34 s	14.6 s	14.7 s	7 min 57 s	7 min 46 s	2 min 29 s	0.016
QBSD	14.3 ms	13.2 ms	13.6 ms	16.4 ms	21.5 ms	8.72 ms	-

The p-values were obtained through a Wilcoxon signed-rank test comparing the particular method with the QBSD results. The alternative hypothesis posits that QBSD results have a faster runtime than the corresponding method being tested.

* All experiments were conducted through their respective Python implementations on a machine with the following specifications: 11th Gen Intel Core i5-1145G7 @ 2.60 GHz, 16 GB RAM.

comparative analysis of the methods across all the mentioned metrics can refer to Table A.5 and Table A.6 in the Appendix. Table 4 shows the execution time of each algorithm for a single training and prediction cycle.

5.1. Statistical Significance

The preference for the Wilcoxon signed-rank test [45] over the paired t-test stems from the non-normal distribution of the difference between the pairs. The paired t-test’s underlying assumption of a normally distributed difference [46] is deemed inapplicable in this context. The p-value signifies the probability of the null hypothesis being true. At a significance level of 5%, a p-value below 0.05 is deemed significant to warrant the rejection of the null hypothesis in favour of the alternative hypothesis.

In Table 3, the null hypothesis proposes that QBSD’s MAPE is equivalent to or exceeds that of the method undergoing comparison. The alternative hypothesis proposes that QBSD demonstrates a MAPE that is significantly lesser than the method being subjected to comparison. The p-values provided in Table 4 share a similar characteristic, with the distinction that the focus is directed towards the comparison of runtimes.

5.2. Forecasting Accuracy

Regarding statistical methodologies, QBSD demonstrates an overall MAPE comparable to SARIMA while exhibiting a statistically significant superiority over Prophet. In specific instances, QBSD outperforms SARIMA, as evidenced in the telecom dataset. However, its effectiveness wanes when capturing data fluctuations within weather datasets. This could potentially arise from QBSD’s design around cyclic patterns, which may not effectively encapsulate the irregular nature of weather patterns.

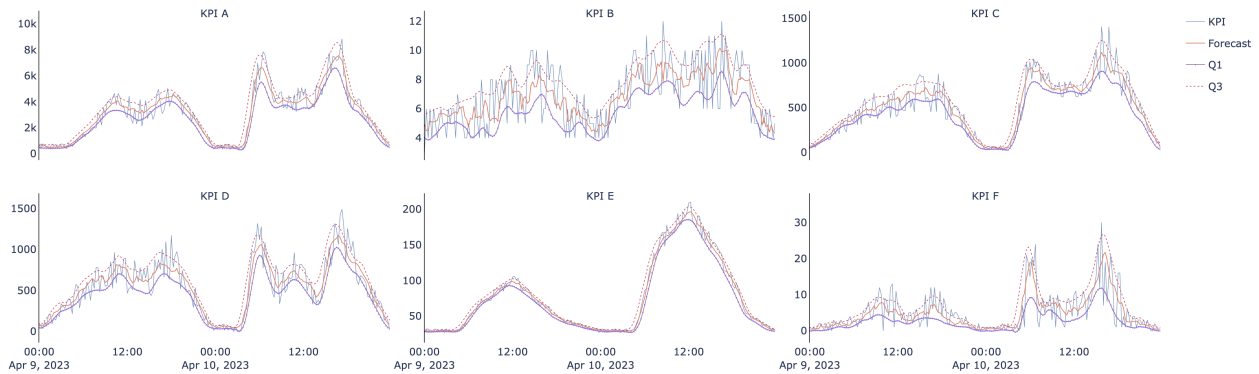


Figure 5: Plot of actual KPI values (A through F) along with forecast, Q_1 , and Q_3 obtained using the QBSD algorithm for the EON1-Cell-F dataset. Series Q_1 and Q_3 have been smoothed with the Savitzky-Golay filter.

Both tree-based approaches notably surpass QBSD in performance. Nonetheless, LightGBM’s under-performance with the Births2015 dataset might be attributed to its constraints in managing datasets with limited data points. According to the evaluation, XGBoost is arguably the method with the least error among all the methods considered in this experiment.

Transitioning to neural forecasting, N-BEATS notably exhibited remarkable performance in the Bitcoin Transactional data skewing the p-value in its favour, despite the MAPE almost paralleling QBSD in other datasets. QBSD consistently achieves a statistically better MAPE compared to N-HiTS across all datasets. It is important to acknowledge that the performance exhibited by neural forecasting methodologies in this experiment might not comprehensively reflect their overall capabilities. The test considers retraining to take place at each step. However, the neural forecasting methods considered are aimed at long-horizon forecasting which is beyond the scope of this study.

In, EON1-Cell-F, QBSD performed similarly to the other best-performing algorithms in accuracy for KPIs A, D, and E. Daily and weekly seasonality was observed in all the presented KPIs, with lower peaks during the weekends due to decreased user activity. Fig. 5 illustrates the ability of QBSD to capture the lower and upper regions of the data for all the KPIs. The bounds Q_1 and Q_3 have been smoothed using the Savitzky-Golay filter (SciPy implementation [47]) for visual aid. Despite the erratic nature of KPI-F, which generated the highest forecasting error, QBSD performed reasonably well in capturing the lower and upper boundaries. For the remaining KPIs, QBSD consistently delivered competitive results.

5.3. Runtime Efficiency

In a practical scenario for telecom systems, for example, a cellular network composed of at least 2000 cells, each cell is characterized by at least 100 KPIs (and even goes above 300 KPIs). In such a system, if anomaly detection is to be applied, there needs to be context-sensitive models deployed for each of these KPIs for each cell. This setup leads to deploying at least 200,000 models that should do both forecasting

and decomposition in addition to anomaly detection. The computational workload would be immense to consider models such as N-BEATS, XGBoost or LightGBM. Not only do these methods incur considerable computational costs, but they also have a much higher space complexity compared to QBSD. Table 4 shows that QBSD has a statistically shorter runtime than the rest of the methods compared. In the observation considering the KPI dataset, QBSD was over 10 times faster than LightGBM, over 25 times faster than XGBoost, and over 22,000 times faster than N-BEATS. These algorithms have a time complexity involving a product of multiple variables depending on the hyperparameter configuration. The marginal benefits the algorithms provide in accuracy cannot satisfy the additional cost in computational complexity. Therefore, in a real-world application, one must make a fair trade-off in accuracy-based metrics for a performance gain in cost.

6. Conclusion

This paper describes QBSD, a computationally effective solution to univariate time series forecasting specialized for RAN KPIs that exhibit seasonality. Though QBSD may not be the best method in terms of forecasting accuracy, it excels in speed while retaining a competitive edge on par with neural forecasting methods. It also produces the time-sensitive upper and lower operating ranges along with the forecast wherein other solutions would have to implement this functionality separately. In practical telecom scenarios with large-scale cellular networks consisting of numerous cells and a substantial number of KPIs, deploying context-sensitive models becomes computationally demanding. Compared to the existing methods, the proposed QBSD demonstrates significantly faster computation, while incurring lower space complexity without a significant loss in forecasting performance. Possible future work can be extending QBSD to model joint distributions between variables for multivariate forecasting.

CRedit authorship contribution statement

Ebenezer RHP Isaac: Conceptualization, Data Curation, Formal Analysis, Investigation, Methodology, Project Administration, Resources, Software, Supervision, Validation, Visualization, Writing - Review & Editing. **Bulbul Singh:** Investigation, Writing - Original Draft, Visualization.

Declaration of competing interest

Ebenezer Isaac is an inventor of the patent filing [14] on which QBSD is based and the ownership of this patent belongs to Ericsson. The authors declare that they have no other known competing financial interests or personal relationships that could have appeared to influence the work reported in this paper.

Declaration of Generative AI and AI-assisted technologies in the writing process

During the preparation of this work, the authors used ChatGPT to improve readability in limited parts of the document. After using this tool, the authors reviewed and edited the content as needed and take full responsibility for the content of the publication.

References

- [1] Y. Ensafi, S. H. Amin, G. Zhang, B. Shah, Time-series forecasting of seasonal items sales using machine learning – a comparative analysis, *International Journal of Information Management Data Insights* 2 (1) (2022) 100058. doi:<https://doi.org/10.1016/j.jjime.2022.100058>.
- [2] T. Hong, P. Pinson, Y. Wang, R. Weron, D. Yang, H. Zareipour, Energy forecasting: A review and outlook, *IEEE Open Access Journal of Power and Energy* 7 (2020) 376–388. doi:[10.1109/OAJPE.2020.3029979](https://doi.org/10.1109/OAJPE.2020.3029979).
- [3] M. Wang, W. Wang, L. Wu, Application of a new grey multivariate forecasting model in the forecasting of energy consumption in 7 regions of China, *Energy* 243 (2022) 123024. doi:<https://doi.org/10.1016/j.energy.2021.123024>.
- [4] M. M. Kumbure, C. Lohrmann, P. Luukka, J. Porras, Machine learning techniques and data for stock market forecasting: A literature review, *Expert Systems with Applications* 197 (2022) 116659. doi:<https://doi.org/10.1016/j.eswa.2022.116659>.
- [5] M. Azadi, S. Yousefi, R. Farzipoor Saen, H. Shabanpour, F. Jabeen, Forecasting sustainability of healthcare supply chains using deep learning and network data envelopment analysis, *Journal of Business Research* 154 (2023) 113357. doi:<https://doi.org/10.1016/j.jbusres.2022.113357>.
- [6] F. Piccialli, F. Giampaolo, E. Prezioso, D. Camacho, G. Acampora, Artificial intelligence and healthcare: Forecasting of medical bookings through multi-source time-series fusion, *Information Fusion* 74 (2021) 1–16. doi:<https://doi.org/10.1016/j.inffus.2021.03.004>.
- [7] A. C. Harvey, *ARIMA Models*, Palgrave Macmillan UK, London, 1990, pp. 22–24. doi:[10.1007/978-1-349-20865-4_2](https://doi.org/10.1007/978-1-349-20865-4_2).
- [8] A. Guin, Travel time prediction using a seasonal autoregressive integrated moving average time series model, in: *2006 IEEE Intelligent Transportation Systems Conference*, 2006, pp. 493–498. doi:[10.1109/ITSC.2006.1706789](https://doi.org/10.1109/ITSC.2006.1706789).
- [9] B. Lim, S. Zohren, Time-series forecasting with deep learning: a survey, *Philosophical Transactions of the Royal Society A* 379 (2194) (2021) 20200209.
- [10] H. Allende, C. Valle, Ensemble methods for time series forecasting, *Claudio Moraga: A passion for multi-valued logic and soft computing* (2017) 217–232.
- [11] H. Zhou, S. Zhang, J. Peng, S. Zhang, J. Li, H. Xiong, W. Zhang, Informer: Beyond efficient transformer for long sequence time-series forecasting, in: *Proceedings of the AAAI conference on artificial intelligence*, Vol. 35, 2021, pp. 11106–11115.
- [12] H. Hewamalage, C. Bergmeir, K. Bandara, Recurrent neural networks for time series forecasting: Current status and future directions, *International Journal of Forecasting* 37 (1) (2021) 388–427. doi:<https://doi.org/10.1016/j.ijforecast.2020.06.008>.
- [13] A. Borovykh, S. Bohte, C. W. Oosterlee, Conditional time series forecasting with convolutional neural networks, arXiv preprint [arXiv:1703.04691](https://arxiv.org/abs/1703.04691) (2017).
- [14] E. R. H. P. Isaac, P. Bhargava, M. Gottumukkala, First node and methods performed thereby for handling anomalous values, Patent No. WO2022271057A1 (June 2021).
URL <https://patents.google.com/patent/WO2022271057A1/>
- [15] SARIMAX.
URL <https://www.statsmodels.org/>

- [16] J. Fattah, L. Ezzine, Z. Aman, H. El Moussami, A. Lachhab, Forecasting of demand using ARIMA model, *International Journal of Engineering Business Management* 10 (2018) 1847979018808673.
- [17] S. J. Taylor, B. Letham, Forecasting at scale, *The American Statistician* 72 (1) (2018) 37–45.
- [18] S. Makridakis, E. Spiliotis, V. Assimakopoulos, A.-A. Semenoglou, G. Mulder, K. Nikolopoulos, Statistical, machine learning and deep learning forecasting methods: Comparisons and ways forward, *Journal of the Operational Research Society* 74 (3) (2023) 840–859. doi:[10.1080/01605682.2022.2118629](https://doi.org/10.1080/01605682.2022.2118629).
URL <https://doi.org/10.1080/01605682.2022.2118629>
- [19] D. Salinas, V. Flunkert, J. Gasthaus, T. Januschowski, DeepAR: Probabilistic forecasting with autoregressive recurrent networks, *International Journal of Forecasting* 36 (3) (2020) 1181–1191. doi:<https://doi.org/10.1016/j.ijforecast.2019.07.001>.
- [20] O. Triebe, H. Hewamalage, P. Pilyugina, N. Laptev, C. Bergmeir, R. Rajagopal, Neuralprophet: Explainable forecasting at scale, *CoRR* abs/2111.15397 (2021). arXiv:2111.15397.
- [21] B. Lim, S. Ö. Arik, N. Loeff, T. Pfister, Temporal fusion transformers for interpretable multi-horizon time series forecasting, *International Journal of Forecasting* 37 (4) (2021) 1748–1764. doi:<https://doi.org/10.1016/j.ijforecast.2021.03.012>.
- [22] S. Li, X. Jin, Y. Xuan, X. Zhou, W. Chen, Y.-X. Wang, X. Yan, Enhancing the locality and breaking the memory bottleneck of transformer on time series forecasting, in: H. Wallach, H. Larochelle, A. Beygelzimer, F. d'Alché-Buc, E. Fox, R. Garnett (Eds.), *Advances in Neural Information Processing Systems*, Vol. 32, Curran Associates, Inc., 2019.
- [23] Y. Zhang, J. Yan, Crossformer: Transformer utilizing cross-dimension dependency for multivariate time series forecasting, in: *The Eleventh International Conference on Learning Representations (ICLR)*, 2022.
- [24] B. N. Oreshkin, D. Carпов, N. Chapados, Y. Bengio, N-beats: Neural basis expansion analysis for interpretable time series forecasting, arXiv preprint arXiv:1905.10437 (2019).
- [25] C. Challu, K. Olivares, B. Oreshkin, F. Garza, M. Mergenthaler, A. Dubrawski, N-hits: Neural hierarchical interpolation for time series forecasting. arxiv, arXiv preprint arXiv:2201.12886 (2022).
- [26] S. Arslan, A hybrid forecasting model using LSTM and prophet for energy consumption with decomposition of time series data, *PeerJ Computer Science* 8 (2022) e1001. doi:<https://doi.org/10.7717/peerj-cs.1001>.
- [27] O. Sprangers, S. Schelter, M. de Rijke, Parameter-efficient deep probabilistic forecasting, *International Journal of Forecasting* 39 (1) (2023) 332–345. doi:<https://doi.org/10.1016/j.ijforecast.2021.11.011>.
- [28] H. Abbasimehr, R. Paki, A. Bahrini, A novel approach based on combining deep learning models with statistical methods for covid-19 time series forecasting, *Neural Computing and Applications* (2022) 1–15.
- [29] G. Zheng, W. K. Chai, J.-L. Duanmu, V. Katos, Hybrid deep learning models for traffic prediction in large-scale road networks, *Information Fusion* 92 (2023) 93–114. doi:<https://doi.org/10.1016/j.inffus.2022.11.019>.
- [30] L. Du, R. Gao, P. N. Suganthan, D. Z. Wang, Bayesian optimization based dynamic ensemble for time series forecasting, *Information Sciences* 591 (2022) 155–175.
- [31] L. R. Berry, P. Helman, M. West, Probabilistic forecasting of heterogeneous consumer transaction–sales time series, *International Journal of Forecasting* 36 (2) (2020) 552–569. doi:<https://doi.org/10.1016/j.ijforecast.2019.07.007>.
- [32] Z. Zeng, M. Li, Bayesian median autoregression for robust time series forecasting, *International Journal of Forecasting* 37 (2) (2021) 1000–1010. doi:<https://doi.org/10.1016/j.ijforecast.2020.11.002>.
- [33] T. Januschowski, Y. Wang, K. Torkkola, T. Erkkilä, H. Hasson, J. Gasthaus, Forecasting with trees, *International Journal of Forecasting* 38 (4) (2022) 1473–1481, special Issue: M5 competition. doi:<https://doi.org/10.1016/j.ijforecast.2021.10.004>.
- [34] G. Ke, Q. Meng, T. Finley, T. Wang, W. Chen, W. Ma, Q. Ye, T.-Y. Liu, LightGBM: A highly efficient gradient boosting decision tree, in: I. Guyon, U. V. Luxburg, S. Bengio, H. Wallach, R. Fergus, S. Vishwanathan, R. Garnett (Eds.), *Advances in Neural Information Processing Systems*, Vol. 30, Curran Associates, Inc., 2017.

- [35] T. Chen, C. Guestrin, XGBoost: A scalable tree boosting system, in: Proceedings of the 22nd ACM SIGKDD International Conference on Knowledge Discovery and Data Mining, KDD '16, Association for Computing Machinery, New York, NY, USA, 2016, p. 785–794. doi:<https://doi.org/10.1145/2939672.2939785>.
- [36] A. Savitzky, M. J. Golay, Smoothing and differentiation of data by simplified least squares procedures., Analytical chemistry 36 (8) (1964) 1627–1639.
- [37] Births2015.
URL <https://www.kaggle.com/datasets/manjusher/births2015>
- [38] A. Kozlov, Daily Electricity Price and Demand Data (2020). doi:10.34740/KAGGLE/DSV/1596730.
URL <https://www.kaggle.com/dsv/1596730>
- [39] S. Kumar, Bitcoin - Transactional Data (2022). doi:10.34740/KAGGLE/DSV/3980973.
URL <https://www.kaggle.com/dsv/3980973>
- [40] D. Dua, C. Graff, UCI machine learning repository (2017).
URL <http://archive.ics.uci.edu/ml>
- [41] Weather.
URL <https://www.ncei.noaa.gov/data/local-climatological-data/>
- [42] Ericsson Research, Ericsson Outlier Nexus (EON), <https://github.com/EricssonResearch/eon>, accessed: 2023-06-27.
- [43] Auto ARIMA.
URL <https://pypi.org/project/pmdarima/>
- [44] Darts Documentation.
URL <https://unit8co.github.io/darts/>
- [45] W. J. Conover, Practical nonparametric statistics, John Wiley & Sons, New York (1971) 97–104.
- [46] J. H. McDonald, Handbook of biological statistics, New York, 2014.
URL <http://www.biostathandbook.com/pairedttest.html>
- [47] P. Virtanen, R. Gommers, T. E. Oliphant, M. Haberland, T. Reddy, D. Cournapeau, E. Burovski, P. Peterson, W. Weckesser, J. Bright, S. J. van der Walt, M. Brett, J. Wilson, K. J. Millman, N. Mayorov, A. R. J. Nelson, E. Jones, R. Kern, E. Larson, C. J. Carey, Í. Polat, Y. Feng, E. W. Moore, J. VanderPlas, D. Laxalde, J. Perktold, R. Cimrman, I. Henriksen, E. A. Quintero, C. R. Harris, A. M. Archibald, A. H. Ribeiro, F. Pedregosa, P. van Mulbregt, SciPy 1.0 Contributors, SciPy 1.0: Fundamental Algorithms for Scientific Computing in Python, Nature Methods 17 (2020) 261–272. doi:10.1038/s41592-019-0686-2.

Appendix A. Detailed Result Tabulation

Table A.5: Comparison of forecasting results on various accuracy metrics

Dataset/method	MSE	RMSE	MAE	MAPE	R^2
<i>Births2015</i>					
Prophet	90735.07	301.223	228.753	2.155	0.974
SARIMA	138396.885	372.017	301.89	2.852	0.96
N-BEATS	35481.620	188.366	146.338	1.384	0.990
XGBoost	41482.788	203.673	121.515	1.11	0.988
LightGBM	3708320.34	1925.7	1701.304	18.287	-0.076
N-HiTS	157355.407	396.68	332.191	3.158	0.954
QBSD	58799.205	242.485	193.304	1.83	0.983
<i>Electricity Demand</i>					
Prophet	167087933.804	12926.25	10606.509	8.5	0.36
SARIMA	231127084.478	15202.864	11390.745	9.329	0.115
N-BEATS	2479207.0	1574.550	1182.520	0.986	0.991
XGBoost	100724795.321	10036.174	4841.364	3.48	0.614
LightGBM	148724999.158	12195.286	9639.455	7.707	0.431
N-HiTS	238457197.415	15442.059	13276.156	11.346	0.087
QBSD	254684088.633	15958.825	12793.552	10.19	0.025
<i>Bitcoin Transactional</i>					
Prophet	377466926.159	19428.508	14518.372	6.598	0.674
SARIMA	504964601.307	22471.417	15897.475	7.062	0.564
N-BEATS	492956200	22202.616	13236.239	5.319	0.574
XGBoost	190717774.713	13810.061	7102.469	2.957	0.835
LightGBM	690626898.834	26279.781	21300.81	9.705	0.404
N-HiTS	1079836411.43	32860.864	25276.649	11.035	0.068
QBSD	444740441.337	21088.87	16285.221	7.419	0.616
<i>Electricity</i>					
Prophet	64109.794	253.199	192.425	6.462	0.554
SARIMA	33213.403	182.245	113.967	3.748	0.769
N-BEATS	86706.893	294.460	231.811	7.228	0.397
XGBoost	7731.313	87.928	35.732	1.021	0.946
LightGBM	38377.163	195.901	119.781	4.171	0.733
N-HiTS	45746.532	213.884	167.355	5.639	0.682
QBSD	50254.254	224.175	163.132	5.294	0.65
<i>Weather</i>					
Prophet	68.431	8.273	7.467	29.750	-1.712
SARIMA	2.120	1.456	0.997	4.610	0.915
N-BEATS	34.191	5.847	4.771	21.354	-0.355
XGBoost	5.356	2.314	1.472	5.381	0.787
LightGBM	12.687	3.562	1.701	11.007	0.497
N-HiTS	36.106	6.009	5.281	21.176	-0.431
QBSD	16.048	4.006	3.084	15.617	0.363

Table A.6: Comparison of forecasting results for EON1-Cell-F.

KPI/Method	MSE	RMSE	MAE	MAPE	R^2
A					
Prophet	1182772.047	1087.553	837.236	39.839	0.727
SARIMA	692267.261	832.026	599.671	19.405	0.84
N-BEATS	369035.420	607.483	467.888	15.413	0.915
XGBoost	254250.218	504.232	242.046	5.464	0.941
LightGBM	422694.707	650.15	358.361	14.92	0.902
N-HiTS	492963.363	702.113	507.212	20.566	0.893
QBSD	404006.097	635.615	479.883	15.702	0.907
B					
Prophet	2.387	1.545	1.292	19.32	0.418
SARIMA	2.636	1.623	1.353	19.912	0.358
N-BEATS	2.144	1.464	1.238	18.376	0.478
XGBoost	1.007	1.004	0.587	6.599	0.755
LightGBM	1.313	1.146	0.812	12.005	0.68
N-HiTS	4.131	2.032	1.589	21.867	0.008
QBSD	2.43	1.559	1.293	18.892	0.408
C					
Prophet	19759.671	140.569	109.989	35.411	0.792
SARIMA	18382.14	135.581	101.174	21.907	0.806
N-BEATS	11613.467	107.766	83.308	18.137	0.878
XGBoost	6404.36	80.027	39.176	5.476	0.932
LightGBM	8668.296	93.104	53.095	13.686	0.909
N-HITS	13903.943	117.915	91.766	31.538	0.868
QBSD	12445.123	111.558	84.828	17.784	0.869
D					
Prophet	31889.494	178.576	141.535	75.767	0.715
SARIMA	29978.605	173.143	135.051	39.819	0.732
N-BEATS	18637.892	136.521	109.982	39.902	0.833
XGBoost	9328.035	96.582	51.005	7.16	0.917
LightGBM	13276.377	115.223	73.89	38.598	0.881
N-HiTS	22240.218	149.131	114.592	52.002	0.869
QBSD	19375.412	139.196	111.798	42.075	0.827
E					
Prophet	373.009	19.313	15.278	26.006	0.879
SARIMA	59.236	7.697	5.656	6.878	0.981
N-BEATS	35.374	5.948	4.593	5.735	0.989
XGBoost	18.177	4.263	2.104	2.14	0.994
LightGBM	45.761	6.765	3.587	4.79	0.985
N-HITS	55.777	7.468	5.539	7.841	0.982
QBSD	33.86	5.819	4.374	5.137	0.989
F					
Prophet	23.709	4.869	3.432	116.839	0.384
SARIMA	24.547	4.954	3.183	83.598	0.362
N-BEATS	18.097	4.254	2.822	75.415	0.530
XGBoost	9.66	3.108	1.327	13.071	0.749
LightGBM	12.194	3.492	1.937	59.796	0.683
N-HITS	26.241	5.122	3.379	108.340	0.318
QBSD	19.491	4.415	2.886	81.881	0.494